Development of a human tissue engineered hypertrophic scar model

van den Broek, L.J.

2015

document version
Publisher's PDF, also known as Version of record

Chapter 6

Tissue engineered human scar models identify extracellular matrix and inflammatory cytokine differences between normotrophic, hypertrophic and keloid scars

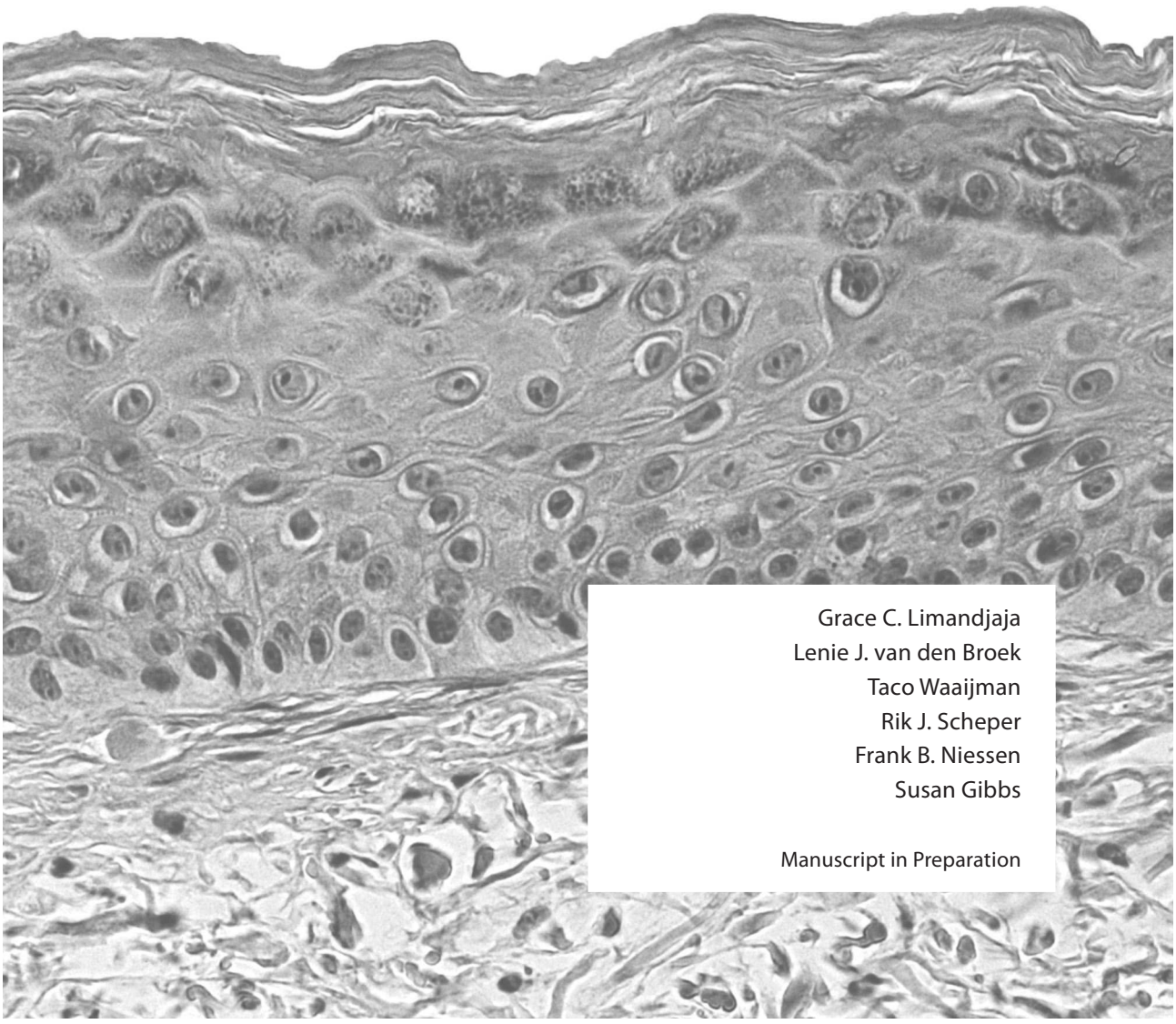

Grace C. Limandjaja
Lenie J. van den Broek
Taco Waaijman
Rik J. Scheper
Frank B. Niessen
Susan Gibbs

Manuscript in Preparation

ABSTRACT

Hypertrophic and keloid scars are the result of unknown abnormalities in the wound healing process. The aim of this study was to develop physiologically relevant, human *in vitro* abnormal scar models for hypertrophic and keloid scars and compare these to normotrophic scars and normal skin to identify differences in the pathogenesis of different scars. Keratinocytes and fibroblasts from normal skin and scars (normotrophic, hypertrophic, keloid) were used to construct skin equivalents (SE). All SE showed normal epidermal differentiation and proliferation. Both abnormal scars showed increased contraction, dermal thickness and myofibroblasts (αSMA) compared to normal skin and normotrophic scar. Notably, the expression of extracellular matrix associated genes showed differential profiles between abnormal scars and normal skin (HGF, HAS1, COL4A2, MMP3) and between the two abnormal scars (IL-18, CCL5, MMP1, ITGA5). Also inflammatory cytokine secretion (CCL5, CXCL1, IL-6, IL-18) was lower in hypertrophic scar compared to normotrophic or keloid scars. Using tissue-engineered scar models we have identified parameters which distinguish normal skin and normotrophic scars from abnormal scars, and hypertrophic scars from keloids.

INTRODUCTION

Hypertrophic and keloid scars are disfiguring scars that can develop after abnormal wound healing. They are characterized by excessive collagen deposition in the dermis and subcutis[1]. These firm, raised scars are not only aesthetically displeasing, but can also cause pruritus, pain, and significant functional disability (e.g. limiting movement)[1-3]. It is extremely difficult to satisfactorily manage these abnormal scars, since recurrence rates are high after excision, in particular for keloids[4].

While differentiation between the hypertrophic and keloid scars can be difficult - especially in younger lesions, important differences do exist between these two types of abnormal scars do exist with respect to prevalence, etiology, onset, growth pattern, maturation/regression, location preference, and the association with contractures. Unlike hypertrophic scars, keloids occur less frequently but show increased prevalence among darker skinned ethnicities[5,6]. Hypertrophic scars are not known to have such an association with race and the risk of hypertrophic scar formation is thought to increase in conjunction with increasing depth of the inciting injury[7]. Keloids usually arise at certain predilection sites such as the trunk and earlobes, while hypertrophic scars have no anatomical association[2,5,8]. Most importantly, the two scars differ with respect to growth and timeline[2,5,8,9]. Hypertrophic scars arise within weeks after the inciting trauma, remain within the boundaries of the original lesion and eventually show some degree of maturation/regression. In contrast, keloids can develop months to years after trauma, are characterized by expansive growth into the surrounding healthy skin and show no or little sign of maturation/regression. Despite these pronounced clinical differences between the two abnormal scar types, a histological distinction remains difficult[10,11]. The presence of whorls of thickened collagen bundles in keloids[8], aptly referred to as 'keloidal collagen' and α-SMA positive myofibroblasts in hypertrophic scars[12,13], have been put forward as distinguishing features. However, α-SMA was found to be present in both scar types[8,14], and while keloidal collagen was rarely seen in hypertrophic scars, it was not always present in all keloid scars[8]. When considering all of the above, it is not surprising that differential diagnosis between both scar types can be very difficult. Nevertheless, the behavioral discrepancies between hypertrophic and keloid scars does strongly suggest that they are two different entities, even though this has not yet been firmly established. In fact, it has been argued that keloids are simply a more aggressive form of hypertrophic scar and that the two are therefore different stages of the same process[5,15].

Despite ongoing research in the field of abnormal wound healing, the pathogenesis underlying either of these hypertrophic and keloid scars remains largely unknown[2,16]. Until the pathogenesis is understood it will remain difficult to develop optimal therapies and to identify novel drug targets for each type of scar. Although abnormalities have

been reported in keratinocytes and fibroblasts derived from these scars[1,6,17-24], there is still no unifying hypothesis to explain how exactly this results in excessive scarring. Unfortunately, research into the pathogenesis of abnormal scar formation has been made difficult by the lack of suitable *in vivo*-like scar models[25]. As these abnormal scars are unique to humans[1], animal models are less than ideal. *In vitro*, monolayers of keratinocytes and fibroblasts derived from scars have frequently been employed[25], but these cultures are missing the essential 3D configuration present in skin. Alternatively, explants of *ex vivo* scars have been sustained in culture for up to six weeks[26-29] and were found to mostly maintain the scar phenotype during this period. While explants obviously provide the most *in vivo*-like scar microenvironment, there is little room for manipulation of experimental variables and the subsequent ability to study the individual effects of the different cell types present in skin and/or involved in wound healing, not to mention the logistical issues with obtaining sufficient samples for experimental testing. Therefore, in this study we developed *in vitro* scar models comprising of scar-derived keratinocytes and fibroblasts cultured to form a fully differentiated epidermis on top of a fibroblast-populated dermal compartment.

Hypertrophic scar were compared with keloid scar models, to determine if there are differences between the tissue types which could point towards differences in the underlying pathological processes. The constructed abnormal scar models were compared to normal skin and normotrophic scars with respect to the following scar parameters: contraction, epidermal and dermal thickness, expression of α-SMA, gene expression of extracellular matrix (ECM) and cellular adhesion-related genes, and secretion of (inflammatory) wound mediators. Previously, we have identified a panel of wound healing mediators that are secreted predominantly by keratinocytes and fibroblasts in skin substitutes[30,31]. These can largely be classified into proteins secreted by keratinocytes (e.g. CCL5, CCL27, VEGF), by fibroblasts (e.g. HGF), or due to crosstalk between keratinocytes and fibroblasts within the full thickness skin equivalents (e.g. CCL2, CXCL1, CXCL8, IL-6). Finally, IL-18 was also included in this panel because it has previously been implicated in keloid formation[32].

The aim of this study was to develop physiologically relevant tissue-engineered scar models which can be used to identify novel differences between normal skin, normal scars and importantly hypertrophic scars and keloids. In the future these models can be used to develop optimal therapies and to identify novel drug targets.

MATERIALS AND METHODS

Normal skin (Nskin), normotrophic scars (NTscar), hypertrophic scars (HTscar) and keloid scars (Kscar) were obtained from the VUmc Plastic Surgery department in compliance

with the 'Code for Proper Secondary Use of Human tissue' in accordance with the declaration of Helsinki. Scars were selected by an experienced scar expert (plastic surgeon) and included only after verbal informed consent. Donor characteristics of the tissue samples used are summarized in Supplement Table 1.

Cell Culture

After washing in phosphate buffered saline, tissue was cut into small fragments and left to incubate in Dispase II solution (Roche Diagnostics, Mannheim, Germany) overnight at 4 °C. Keratinocytes and fibroblasts were isolated and cultured as described previously[7]. Cells were cryopreserved in liquid nitrogen when (P0) cultures were approximately 80% confluent and stored until later assembly into skin equivalents.

Cell culture and construction of skin equivalents

Skin equivalents (SE) were constructed in duplicate from keratinocytes and fibroblasts derived from normal skin (n=8 donors), normotrophic scars (n=6 donors), hypertrophic scars (n=5 donors) and keloid scars (n=7 donors) essentially as previously described[7]. In brief, $4x10^5$ fibroblasts were seeded onto 2.2 x 2.2cm squares of Matriderm® (dr. Suwelack Skin & Health Care, Billerbeck, Germany) and cultured for 3 weeks in a 37°C, 5% CO_2 atmosphere. Keratinocytes (P2) were then seeded on top of the sheets and cultured submerged for 3-4 days prior to culturing at an air-liquid interface for an additional 10 days. Upon addition of keratinocytes, SE were cultured in a 37°C, 7.5% CO_2 atmosphere. Medium was changed twice a week.

Wound contraction

Wound contraction was expressed as a reduction in surface area of the SE at the end of the culture period. Surface area (mm^2) was determined from photographs of the constructs when SE were harvested (week 5), using NIS-Elements AR 2.10 imaging software (Nikon).

Histological analysis

Paraffin tissue sections (5µm) were stained with Haematoxylin and Eosin for histologic evaluation and determination of epidermal and dermal thickness. Epidermal thickness was determined by counting the number of keratinocyte cell layers at 3 random points in the SE sections at a 200x magnification. Thickness of the dermis was measured using NIS-elements software to calculate length in µm at 5 random points in a 100x magnification.

Immunohistochemical staining

Immunohistochemical stainings were performed on deparaffinized, formalin-fixed tissue sections to assess epidermal proliferation (Ki67: clone MIB-1, Dakocytomation, Glostrup, Denmark; 1:50), epidermal differentiation (keratin 10/K10: clone DE-K10, Progen, Heidelberg, Germany; 1:500), presence of fibroblasts (vimentin: clone V9, Dakocytmation, Glostrup, Denmark) and myofibroblasts (α-SMA: clone 1A4, Dakocytomation, Glostrup, Denmark). Supplementary antigen retrieval treatments were performed prior to incubation with the primary antibody using a 15 min. incubation step with pepsin (K10) and/or heat-induced antigen retrieval with 0.01M citrate buffer pH 6.0 (Ki67, K10, vimentin).

Scoring of Immunohistochemical staining: (–) absence of staining; (+) normal staining pattern; (++) increased number of positively stained cells; (+++) strongly increased number of positively stained cells.

Ki67 Proliferation index: at a 100x magnification in three random locations in a tissue section, 100 basal cells were counted. The proliferation index was defined as the percentage of Ki67 positive nuclei within these regions.

Enzyme-linked immunosorbent assay

Culture supernatants (1.5 ml) derived from SE were collected over a 24-hour period at the end of the culture period (week 5) to measure the levels of IL-18 (MBL International, Woburn, Massachusetts, USA); IL-6 and CXCL8 (PeliKine Sanguin Reagents, Amsterdam, The Netherlands); CCL2, CCL5, CCL20, CCL27, CXCL1, HGF and VEGF (R&D System Inc., Minneapolis, Minnesota, USA) secreted by the SE, using enzyme-linked immunosorbent assays (ELISA) essentially as described by the suppliers.

Modified qPCR array of ECM and cellular adhesion-related genes

For RNA isolation, the epidermis was separated from the dermis using a slide-warmer (40 ^{o}C) followed by immediate freezing in liquid nitrogen until further processing. Epidermis and dermis samples were disrupted and homogenized in the TissueLyser LT/II (Qiagen, Hilden, Germany). RNA isolation was performed using QiaShredder™ kits and RNeasy® Mini kits with on-column DNAse digestion. cDNA was synthesized using the RT^2 First Strand Kit, while the RT^2 SYBR Green Fluor qPCR Mastermix was used to run a modified RT^2 Profiler PCR array 'Human Extracellular Matrix and Adhesion Molecules' (PAHS-013A) with 86 genes of interest in a Bio-rad iCycler (Bio-rad Laboratories Inc., Hercules, CA, USA). This array was adapted to include two additional genes, collagen III and elastin (see Supplementary Table 2 and 3). The geometric mean of two housekeeping genes: β-Actin (ACTB; NM_001101) and Hypoxanthine phosphoribosyltransferase 1 (HPRT1; NM_000194), was used to normalize expression. All RNA and qPCR reagents were obtained from Qiagen, Hilden, Germany.

MTT assay

A colorimetric (MTT based) assay was used to quantify cell proliferation and viability (Roche Applied Science, Penzberg, Germany) of the SE, as described previously[33].

Data analysis

Experiments were performed in duplicate with at least n=5 different donors, all results are expressed as the mean ± SEM. GraphPad Prism 6 software (MacKiev) was used to construct graphs and to perform statistical analysis. Comparisons were performed using Mann-Whitney tests, testing a total of 6 comparisons without correction for multiple comparisons. For analysis of the PCR data, gene expression ($2^{-\Delta Ct}$) was normalized with the geometric mean of two housekeeping genes (ACTB and HRPT1). Shapiro-Wilk normality tests confirmed the presence of a normal distribution, thus justifying the use of one-way ANOVA's to detect which genes showed significant differences between the four experimental groups. Post-hoc Tukey's HSD tests were performed for pair-wise comparisons. Differences were considered significant if $p<0.05$ (*), $p<0.01$ (**) or $p<0.001$ (***).

RESULTS

Hypertrophic and keloid scar model show increased contraction and dermal thickness compared to normal skin and normal scar

In order to determine in how far our tissue-engineered scar models represented their native counterparts, we first compared the different types of *in vitro* cultured scars with regards to contraction and dermal thickness (Figure 1). In line with their native counterparts, both the hypertrophic (HTscar) and keloid scar (Kscar) models showed significantly more contraction compared to normal skin and normotrophic scar (Figure 1a). Furthermore, it was found that the thickness of HTscar and Kscar were significantly greater than that of either NTscar or Nskin and that the thickness of Nskin and NTscar were similar (Figure 1b). In contrast to dermal thickness, no difference was observed between epidermal thickness between the different scar models (data not shown).

Increased α-SMA expression in central deep keloid scars

All SE possessed a fully differentiated epidermis located on top of a fibroblast-populated dermis (Figure 2). The SE were further characterized with the aid of immunohistochemistry for the presence of fibroblasts (vimentin) and myofibroblasts (α-SMA) (Table 1). While there was little staining for α-SMA in Nskin and NTscar, positive staining was clearly present in HTscar and Kscar. Vimentin which stains all fibroblasts showed that equal numbers of fibroblasts were present in all the skin equivalents. Next the expression of epidermal proliferation (Ki67) and differentiation (keratin 10) biomarkers was determined (Table 1).

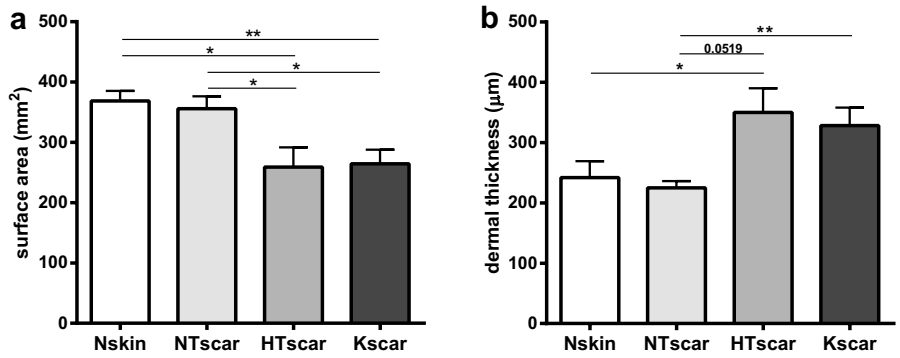

Figure 1. Increased contraction and dermal thickness in hypertrophic and keloid scars models. (**a**) Both abnormal scars showed significantly decreased surface areas, and thereby increased contraction, compared to Nskin and NTscar. Contraction was measured as a reduction in end surface area (mm^2) after 5 weeks of culturing. (**b**) Dermal thickness was increased in both abnormal scars compared to normal skin and normal scar SEs. Experiments (Nskin (n=8), NTscar (n=6), HTscar (n=5), Kscar (n=7)) were performed with intra-experimental duplicates for each donor which represents an independent experiment and shown as mean ± SEM. Data were analysed with Mann-Whitney U tests and differences between the experimental groups were considered statistically significant if $*p<0.05$ or $**p<0.01$.

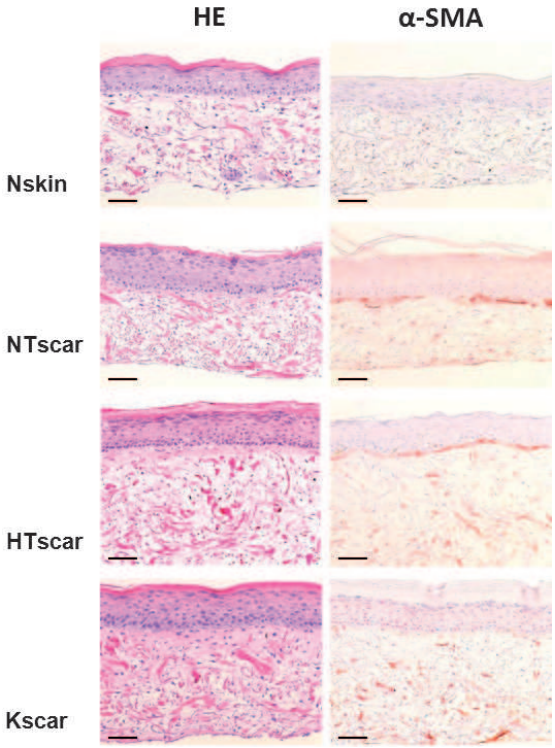

Figure 2. Representative pictures showing hematoxylin/eosin (HE) and α-SMA stainings of skin equivalents. Nskin, NTscar, HTscar and Kscar are shown. Bar = 100µm

Table 1. Immunohistochemical stainings of skin equivalents

Marker	Nskin	NTscar	HTscar	Kscar
EPIDERMIS				
Ki67 Proliferation	13.1 ± 4.5	13.5 ± 4.8	16.6 ± 7.9	18.8 ± 4.8
Keratin 10 Differentiation	SPB	SPB	SPB	SPB
DERMIS				
Vimentin Fibroblasts	+	+	+	+
α-SMA Myofibroblasts	– (1/7) +/– (4/7) + (1/7) ++ (1/7)	+/– (3/4) ++ (1/4)	+ (3/5) ++ (1/5) +/– (1/5)	+ (3/4) +++ (1/4)

The results of immunohistochemical stainings of epidermal markers (Ki67, keratin 10) and dermal fibroblast markers (vimentin, α-SMA) in SE of Nskin (n=7), NTscar (n=4), HTscar (n=5) and Kscar (n=4). Ki67 is expressed as mean ± SD; SPB: suprabasal expression; –, absent; +/–, minimal expression; +, normal expression; ++, increased expression; +++, strongly increased expression.

There was no significant difference in the number of Ki67-positive proliferating cells between the different scar models. Also a normal suprabasal keratin 10 expression was observed in all groups.

Taken together these results show that the tissue-engineered scar models closely resembled their native counterparts in that HTscar and Kscar showed increased contraction, dermal thickness and α-SMA expression compared to Nskin and Nscar, thus making them a valid tool to investigate novel differences between HTscar and Kscar.

Differential expression of ECM-related genes between the different tissue types

Since the *in vitro* scar models closely resembled their native counterparts they provide a novel means to identify differences between NTscar and HTscar or Kscar and most importantly differences between HTscar and Kscar. First we compared the expression of ECM and cell adhesion related genes in the different *in vitro* scar models with the aid of a modified qPCR array (Supplement Table 2 and 3). Differential expression between the scar models with respect to genes involved in basement membrane deposition (LAMA1, COL4A2), cell-matrix adhesion (ITGA5), ECM synthesis (HAS1) and ECM breakdown (MMP1, MMP3) was observed (Figure 3 and Supplement Table 4). With regards to the epidermal compartment, there was a clear increase in expression of the basement membrane protein laminin (LAMA1) in Nscar compared to Nskin or Kscar whereas in the dermal compartment the basement membrane protein collagen IV (COL4A2) expression decreased with increasing extent of scar severity. Expression of hyaluronan synthase (HAS1) (an enzyme that produces the polysaccharide hyaluronan) and MMP3 genes, were also decreased in the dermal compartment of all scars. Notably two genes (ITGA5

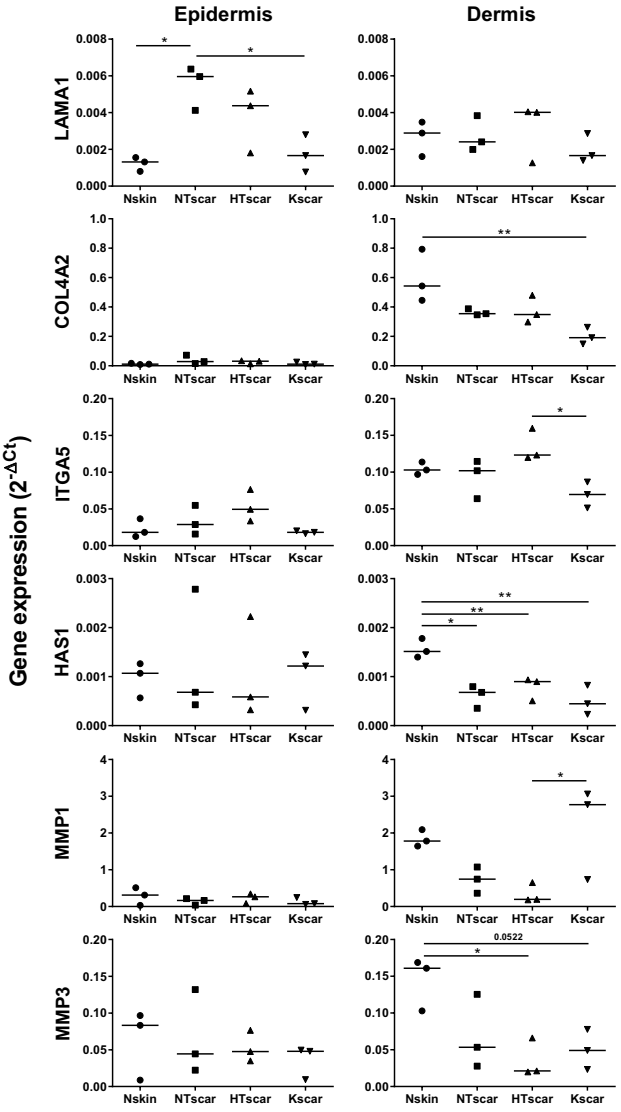

Figure 3. Differential expression of ECM-related genes between the different skin equivalents. Normalized gene expression of LAMA1, COL4A2, ITGA5, HAS1, MMP1 and MMP3 in the epidermis and dermis is expressed as $2^{\wedge-(\Delta Ct)}$ of SE for Nskin, NTscar, HTscar and Kscar n=3 donors for each scar type. Data were analyzed with one-way ANOVA's to detect which genes showed significant differences between the four experimental groups. Post-hoc Tukey's HSD tests were performed for pair-wise comparisons. Differences were considered significant if $p<0.05$ (*) or $p<0.01$(**).

and MMP1) showed differential expression in the HTscar and Kscar. Whereas cell matrix adhesion gene ITGA5 was decreased in Kscar compared to HTscar, MMP1 was increased in Kscar compared to HTscar. This differential expression pattern lends further support to the hypothesis that hypertrophic scars and keloids are truly different entities.

Differential inflammatory cytokine and growth factor secretion distinguishes keloid scars from hypertrophic scars

Next we compared the secretion profile of a panel of inflammatory cytokines and growth factors known to be involved in wound healing (Figure 4). Three different secretion profiles were observed in which proteins showed a) decreased secretion in

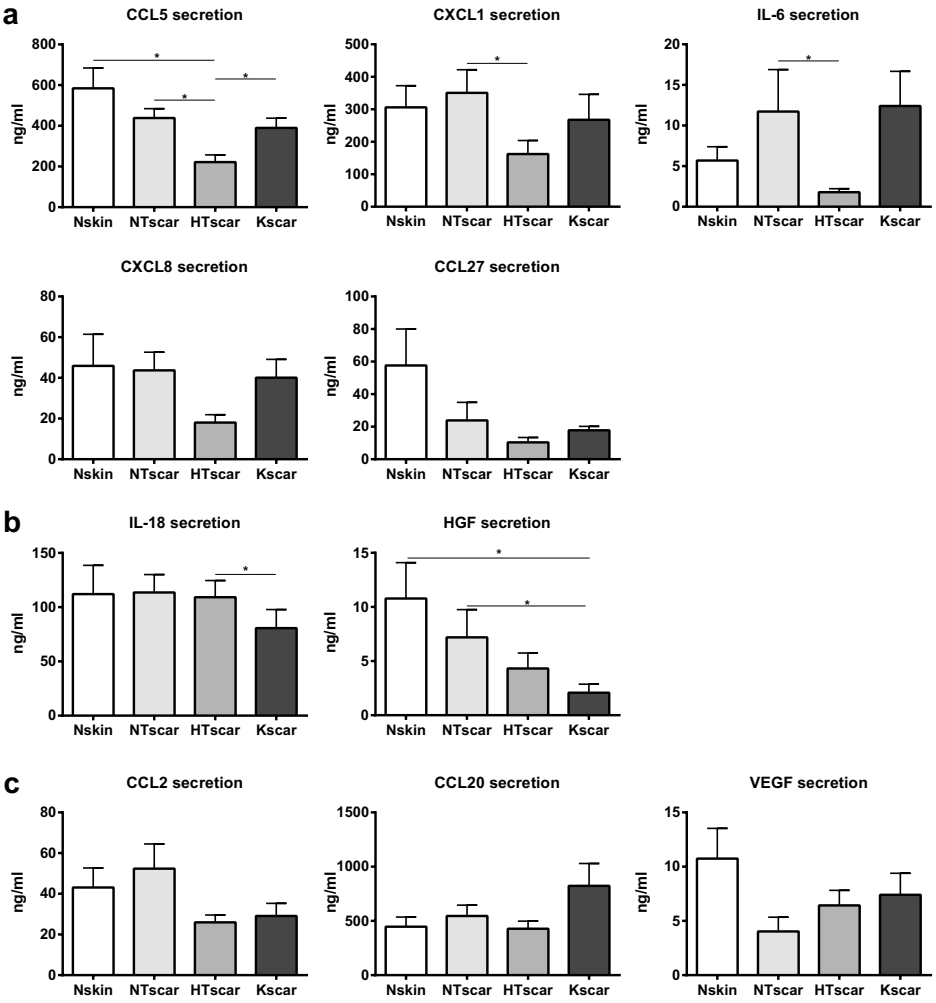

Figure 4. Differential inflammatory cytokine and growth factor secretion distinguishes abnormal scars from normal skin and keloids from hypertrophic scars. Wound healing mediator secretion was determined in SE derived from Nskin (n=8), NTscar (n=6), HTscar (n=5), Kscar (n=7). (**a**) Inflammatory mediators increased in HTscar compared to Kscar (**b**) Mediators decreased in HTscar compared to Kscar (**c**) Similar secretion of mediators between different SE. Experiments were performed in duplicate and shown as mean ± SEM in ng/ml. Data were analyzed with Mann-Whitney U tests and differences between the experimental groups were considered statistically significant if *p<0.05.

HTscar compared to Kscar and NTscar (CCL5, CXCL1, IL-6, CXCL8 (trend), CCL27 (trend)), b) decreased secretion in Kscar compared to HTscar and NTscar (IL-18, HGF), or c) no difference between the 3 scar types . In all cases the secretion profile of Nskin was similar to that of Nscar . The differences in secretion levels of the above mentioned factors was not the result of a difference in viability, as MTT values were not significantly different between groups (graph not shown).

DISCUSSION

Using full thickness human scar models derived from keratinocytes and fibroblasts isolated from different scar types (NTscar, HTscar, Kscar), we were able to identify novel parameters to distinguish these different scar types. All abnormal scars (HTscar and Kscar) showed increased contraction, dermal thickness and α-SMA expression compared to Nskin and NTscar. However, HTscar and Kscar differed with respect to inflammatory cytokine and growth factor secretion and expression of ECM associated genes.

Contraction of the SE was increased in both abnormal scars compared to Nskin and NTscar in conjunction with increased numbers of myofibroblasts. Contractures are typically associated with hypertrophic scar formation and increased contraction has also previously been demonstrated *in vitro* in 3D cultures of both hypertrophic- and keloid-derived fibroblasts[9,34-39]. Conflicting results have been reported with respect to α-SMA staining. It has been described both as a distinguishing feature of hypertrophic scars[12] and as being present in both abnormal scars[14]. Our results are in line with Lee et al.[14] who also found positive α-SMA staining in keloids. It should be noted that neither the contraction nor the staining was the result of differences in the quantity of fibroblasts in the SE, as the vimentin staining was similar in each of the models.

In addition to increased contraction, we found increased dermal thickness in both HTscar and Kscar models compared to Nskin and NTscar. While the increase was significant and corresponding with the *in vivo* increased matrix deposition[1], it was not in the same order of magnitude as the *in vivo* scars. However, it should be noted that the SE are formed over a period of only 5 weeks, whereas keloid and hypertrophic scars normally start to develop at the earliest 4 weeks after injury[7]. In line with the increased dermal thickness, differences were observed between the expression of ECM genes in the different scar models. It was found that LAMA1 (basement membrane gene) increased in SE of NTscar compared to Nskin and Kscar. In contrast another basement membrane gene (COL4A2) was decreased in the Kscar model compared to Nskin. The decreased expression of HAS1 and MMP3 in the scar models compared to Nskin was in line with decreased expression of HAS1 in *in vivo* scars[24] and decreased expression of MMP3 in scar-derived fibroblasts[40,41]. This suggest that the ECM differs in our *in vitro* scars when compared to

our *in vitro* Nskin model which is in line with *in vivo* data[24]. Taken together, these data indicate that the *in vitro* scar models closely resemble their native counterparts and can therefore be used to identify novel differences between the different scar types.

Interestingly two ECM related genes (ITGA5 and MMP1) were differently expressed in SE of HTscar and Kscar. ITGA5 is part of one of the integrin's which bind to fibronectin[42] and fibronectin is known to be increased in both adverse scars compared to normal skin[24]. The decreased expression of ITGA5 in SE of Kscars compared to SE of HTscars suggests that even though fibronectin may not be differently expressed, the adhesion of integrins fibronectin may differ between these adverse scars. The differential expression of MMP1 gene expression in the HTscar and Kscar models is not in line with the finding that both hypertrophic scar and keloid derived fibroblast cultures show decreased expression of MMP1 compared to normal skin derived fibroblast[40,43] However our 3D organotypic model consists of both fibroblasts and keratinocytes and it has been described that factors secreted by keratinocytes can induce expression of MMP1 in fibroblasts[44] and that keratinocytes can also produce MMP1[45]. Taken together, this emphasizes the benefit of using physiologically relevant human models to identify differences between hypertrophic scars and keloid scars.

HTscar and Kscar also showed differences in the secretion of inflammatory cytokines and growth factors. Notably only HTscar, but not Kscar, showed decreased secretion levels of several inflammatory mediators (IL-6, CXCL8, CXCL1, CCL5 and CCL27) compared to NTscar. Previously we have shown in a hypertrophic scar model composed of a reconstructed epidermis on an adipose tissue-derived mesenchymal stem cells populated dermal matrix that IL-6 and CXCL8 secretion was also decreased compared to scar models containing dermal fibroblasts, which is in line with these current findings[7]. Cytokine IL-18 showed decrease secretion in Kscar compared to HTscar (significant) and NTscar (trend) in line with *in vivo* keloid scar data which also showed decreased levels of IL-18 compared to normal skin[32]. Similar MTT values and secretion of some factors (CCL2, CCL20 and VEGF) make it unlikely that our observed differences described above are the result of differences in metabolic activity in the different scar models. In contrast to the differential expression between adverse scar types of the above mentioned inflammatory factors, expression of the HGF decreased with increasing severity of the scar type in line with its previously reported anti-fibrotic properties[46,47].

In summary, we have demonstrated that keratinocytes and fibroblasts derived from scars can be cultured *in vitro* to form full thickness skin equivalents mimicking *in vivo* scar tissues. We have identified specific differences between the different types of scars and also between healthy skin. Increased contraction, dermal thickness and α-SMA expression were abnormal scar parameters observed in both HTscar and Kscar. However, the differential secretion and gene expression patterns of inflammatory cytokines, growth factors and ECM proteins strongly suggests that abnormal scars arise from dif-

ferent pathologies rather than simply being on different ends of the scarring spectrum. This is supported by their clinical differences with respect to growth pattern and natural progression over time . For this reason, we emphasize the importance of maintaining a clear distinction between HTscar and Kscar in research, and encourage the inclusion of all scar types (NTscar, HTscar and Kscar) and Nskin in studies using physiologically relevant human scar models to generate a more comprehensive understanding of scar tissue formation. This is ultimately required to develop optimal treatment strategies and to identify novel drug targets.

ACKNOWLEDGEMENTS

The authors would like to thank W. van Wieringen for assistance with statistical analysis of the qPCR array data, H. W. van Essen for technical assistance with the qPCR arrays and M. Breetveld and S. C. Sampat-Sardjoepersad for practical assistance.

REFERENCES

1. Tuan T L, Nichter L S The molecular basis of keloid and hypertrophic scar formation. Mol Med Today 1998: 4: 19-24.
2. Seifert O, Mrowietz U Keloid scarring: bench and bedside. Arch Dermatol Res 2009: 301: 259-272.
3. Shih B, Garside E, McGrouther D A et al. Molecular dissection of abnormal wound healing processes resulting in keloid disease. Wound Repair Regen 2010: 18: 139-153.
4. Mustoe T A, Cooter R D, Gold M H et al. International clinical recommendations on scar management. Plast Reconstr Surg 2002: 110: 560-571.
5. Burd A, Huang L Hypertrophic response and keloid diathesis: two very different forms of scar. Plast Reconstr Surg 2005: 116: 150e-157e.
6. Wolfram D, Tzankov A, Pulzl P et al. Hypertrophic scars and keloids--a review of their pathophysiology, risk factors, and therapeutic management. Dermatol Surg 2009: 35: 171-181.
7. van den Broek L J, Niessen F B, Scheper R J et al. Development, validation and testing of a human tissue engineered hypertrophic scar model. ALTEX 2012: 29: 389-402.
8. Robles D T, Berg D Abnormal wound healing: keloids. Clin Dermatol 2007: 25: 26-32.
9. Butler P D, Ly D P, Longaker M T et al. Use of organotypic coculture to study keloid biology. Am J Surg 2008: 195: 144-148.
10. Rossiello L, D'Andrea F, Grella R et al. Differential expression of cyclooxygenases in hypertrophic scar and keloid tissues. Wound Repair Regen 2009: 17: 750-757.
11. Verhaegen P D, van Zuijlen P P, Pennings N M et al. Differences in collagen architecture between keloid, hypertrophic scar, normotrophic scar, and normal skin: An objective histopathological analysis. Wound Repair Regen 2009: 17: 649-656.
12. Ehrlich H P, Desmouliere A, Diegelmann R F et al. Morphological and immunochemical differences between keloid and hypertrophic scar. Am J Pathol 1994: 145: 105-113.
13. Kose O, Waseem A Keloids and hypertrophic scars: are they two different sides of the same coin? Dermatol Surg 2008: 34: 336-346.
14. Lee J Y, Yang C C, Chao S C et al. Histopathological differential diagnosis of keloid and hypertrophic scar. Am J Dermatopathol 2004: 26: 379-384.
15. Kischer C W Comparative ultrastructure of hypertrophic scars and keloids. Scan Electron Microsc 1984: 423-431.
16. Slemp A E, Kirschner R E Keloids and scars: a review of keloids and scars, their pathogenesis, risk factors, and management. Curr Opin Pediatr 2006: 18: 396-402.
17. Funayama E, Chodon T, Oyama A et al. Keratinocytes promote proliferation and inhibit apoptosis of the underlying fibroblasts: an important role in the pathogenesis of keloid. J Invest Dermatol 2003: 121: 1326-1331.
18. Hakvoort T E, Altun V, Ramrattan R S et al. Epidermal participation in post-burn hypertrophic scar development. Virchows Arch 1999: 434: 221-226.
19. Khoo Y T, Ong C T, Mukhopadhyay A et al. Upregulation of secretory connective tissue growth factor (CTGF) in keratinocyte-fibroblast coculture contributes to keloid pathogenesis. J Cell Physiol 2006: 208: 336-343.
20. Lim I J, Phan T T, Song C et al. Investigation of the influence of keloid-derived keratinocytes on fibroblast growth and proliferation in vitro. Plast Reconstr Surg 2001: 107: 797-808.
21. Lim I J, Phan T T, Bay B H et al. Fibroblasts cocultured with keloid keratinocytes: normal fibroblasts secrete collagen in a keloidlike manner. Am J Physiol Cell Physiol 2002: 283: C212-C222.

22. Phan T T, Lim I J, Bay B H et al. Differences in collagen production between normal and keloid-derived fibroblasts in serum-media co-culture with keloid-derived keratinocytes. J Dermatol Sci 2002: 29: 26-34.
23. Rockwell W B, Cohen I K, Ehrlich H P Keloids and hypertrophic scars: a comprehensive review. Plast Reconstr Surg 1989: 84: 827-837.
24. Sidgwick G P, Bayat A Extracellular matrix molecules implicated in hypertrophic and keloid scarring. J Eur Acad Dermatol Venereol 2012: 26: 141-152.
25. van den Broek L J, Limandjaja G C, Niessen F B et al. Human hypertrophic and keloid scar models: principles, limitations and future challenges from a tissue engineering perspective. Exp Dermatol 2014: 23: 382-386.
26. Bagabir R, Syed F, Paus R et al. Long-term organ culture of keloid disease tissue. Exp Dermatol 2012: 21: 376-381.
27. Ehrlich H P, Buttle D J Epidermis promotion of collagenase in hypertrophic scar organ culture. Exp Mol Pathol 1984: 40: 223-234.
28. Junker J P, Kratz C, Tollback A et al. Mechanical tension stimulates the transdifferentiation of fibroblasts into myofibroblasts in human burn scars. Burns 2008: 34: 942-946.
29. Kratz C, Tollback A, Kratz G Effects of continuous stretching on cell proliferation and collagen synthesis in human burn scars. Scand J Plast Reconstr Surg Hand Surg 2001: 35: 57-63.
30. Spiekstra S W, Breetveld M, Rustemeyer T et al. Wound-healing factors secreted by epidermal keratinocytes and dermal fibroblasts in skin substitutes. Wound Repair Regen 2007: 15: 708-717.
31. van den Broek L J, Kroeze K L, Waaijman T et al. Differential response of human adipose tissue-derived mesenchymal stem cells, dermal fibroblasts, and keratinocytes to burn wound exudates: potential role of skin-specific chemokine CCL27. Tissue Eng Part A 2014: 20: 197-209.
32. Do D V, Ong C T, Khoo Y T et al. Interleukin-18 system plays an important role in keloid pathogenesis via epithelial-mesenchymal interactions. Br J Dermatol 2012: 166: 1275-1288.
33. Waaijman T, Breetveld M, Ulrich M et al. Use of a collagen-elastin matrix as transport carrier system to transfer proliferating epidermal cells to human dermis in vitro. Cell Transplant 2010: 19: 1339-1348.
34. Chiu L L, Sun C H, Yeh A T et al. Photodynamic therapy on keloid fibroblasts in tissue-engineered keratinocyte-fibroblast co-culture. Lasers Surg Med 2005: 37: 231-244.
35. Kamamoto F, Paggiaro A O, Rodas A et al. A wound contraction experimental model for studying keloids and wound-healing modulators. Artif Organs 2003: 27: 701-705.
36. Mukhopadhyay A, Tan E K, Khoo Y T et al. Conditioned medium from keloid keratinocyte/keloid fibroblast coculture induces contraction of fibroblast-populated collagen lattices. Br J Dermatol 2005: 152: 639-645.
37. Phan T T, Sun L, Bay B H et al. Dietary compounds inhibit proliferation and contraction of keloid and hypertrophic scar-derived fibroblasts in vitro: therapeutic implication for excessive scarring. J Trauma 2003: 54: 1212-1224.
38. Sahara K, Kucukcelebi A, Ko F et al. Suppression of in vitro proliferative scar fibroblast contraction by interferon alfa-2b. Wound Repair Regen 1993: 1: 22-27.
39. Tsai C, Hata K, Torii S et al. Contraction potency of hypertrophic scar-derived fibroblasts in a connective tissue model: in vitro analysis of wound contraction. Ann Plast Surg 1995: 35: 638-646.
40. McFarland K L, Glaser K, Hahn J M et al. Culture medium and cell density impact gene expression in normal skin and abnormal scar-derived fibroblasts. J Burn Care Res 2011: 32: 498-508.

41. Li Y, Kilani R T, Rahmani-Neishaboor E et al. Kynurenine increases matrix metalloproteinase-1 and -3 expression in cultured dermal fibroblasts and improves scarring in vivo. J Invest Dermatol 2014: 134: 643-650.
42. Adkison L R, White R A, Haney D M et al. The fibronectin receptor, alpha subunit (Itga5) maps to murine chromosome 15, distal to D15Mit16. Mamm Genome 1994: 5: 456-457.
43. Uchida G, Yoshimura K, Kitano Y et al. Tretinoin reverses upregulation of matrix metalloproteinase-13 in human keloid-derived fibroblasts. Exp Dermatol 2003: 12 Suppl 2: 35-42.
44. Ghahary A, Marcoux Y, Karimi-Busheri F et al. Differentiated keratinocyte-releasable stratifin (14-3-3 sigma) stimulates MMP-1 expression in dermal fibroblasts. J Invest Dermatol 2005: 124: 170-177.
45. Pilcher B K, Dumin J A, Sudbeck B D et al. The activity of collagenase-1 is required for keratinocyte migration on a type I collagen matrix. J Cell Biol 1997: 137: 1445-1457.
46. Mukhopadhyay A, Fan S, Dang V D et al. The role of hepatocyte growth factor/c-Met system in keloid pathogenesis. J Trauma 2010: 69: 1457-1466.
47. Naim R, Naumann A, Barnes J et al. Transforming growth factor-beta1-antisense modulates the expression of hepatocyte growth factor/scatter factor in keloid fibroblast cell culture. Aesthetic Plast Surg 2008: 32: 346-352.

SUPPLEMENT CHAPTER 6

Supplement table 1: Tissue and donor characteristics

SCAR CHARACTERISTICS				DONOR CHARACTERISTICS		
Donor	**Location of origin**	**Previous treatment**	**Etiology**	**Skin color**	**Age**	**Gender**
Nskin 1	Breast	NA	NA	White	40 yr	Male
Nskin 2	Breast	NA	NA	White	34 yr	Male
Nskin 3	Abdomen	NA	NA	Dark brown	?	Female
Nskin 4	Abdomen	NA	NA	White	59 yr	Female
Nskin 5	Abdomen	NA	NA	?	49 yr	Female
Nskin 6	Breast	NA	NA	Dark brown	30 yr	Female
Nskin 7	Lower extremity	NA	NA	White	?	?
Nskin 8	Abdomen	NA	NA	Dark brown	39 yr	Female
NTscar 1	?	?	?	White	38 yr	Female
NTscar 2	Breast	?	?	White	56 yr	Female
NTscar 3	Abdomen	?	?	Brown	30 yr	Female
NTscar 4	Back	None	Surgical procedure	White	40 yr	Female
NTscar 5	Lower extremity	None	Dog bite	Brown	51 yr	Male
NTscar 6	Flank	None	Surgical procedure	White	58 yr	Female
HTscar 1	?	?	?	Brown	39 yr	Female
HTscar 2	?	?	?	White	17 yr	Female
HTscar 3*	Abdomen	?	?	Dark brown	22 yr	Male
HTscar 4	Abdomen	?	?	Dark brown	24 yr	Male
HTscar 5*	?	?	?	Dark brown	?	Male
HTscar 6	Sternum	Corticosteroids	Surgical procedure	Brown	?	Female
HTscar 7	Abdomen	Corticosteroids	Surgical procedure	White	40 yr	Female
Kscar 1	Earlobe	None	Piercing	Dark brown	20 yr	Male
Kscar 2	Breast	Excision; Silicone; Corticosteroids	Surgical procedure	Dark brown	64 yr	Female
Kscar 3	Shoulder	Corticosteroids	Acne	Dark brown	40 yr	Female
Kscar 4	Sternum	Corticosteroids; Laser	?	Brown	28 yr	Female
Kscar 5	Retro-auricular	Excision; Corticosteroids	Surgical procedure	Dark brown	49 yr	Male
Kscar 6	Abdomen	?	?	Dark brown	39 yr	Female
Kscar 7	Breast	None	Surgical procedure	Dark brown	43 yr	Female

Overview of the characteristics of the tissue used for this study. All skin equivalents (SE) were constructed using donor matched keratinocytes and fibroblasts, except for one of the hypertrophic scar SE (depicted with *, here the fibroblasts of donor 3 were used with the keratinocytes of donor 5 to construct the SE). NA: not applicable, ?: unknown. All scars used were at least one year old and had matured, keloid scars were usually longstanding and up to 12 years old.

Supplement table 2: Overview of genes tested

Cell Adhesion Molecules
Transmembrane Molecules: CD44, CDH1, HAS1, ICAM1, ITGA1, ITGA2, ITGA3, ITGA4, ITGA5, ITGA6, ITGA7, ITGA8, ITGAL, ITGAM, ITGAV, ITGB1, ITGB2, ITGB3, ITGB4, ITGB5, MMP14, MMP15, MMP16, NCAM1, PECAM1, SELE, SELL, SELP, SGCE, SPG7, VCAM1.
Cell-Cell Adhesion: CD44, CDH1, COL11A1, COL14A1, COL6A2, CTNND1, ICAM1, ITGA8, VCAM1.
Cell-Matrix Adhesion: ADAMTS13, CD44, ITGA1, ITGA2, ITGA3, ITGA4, ITGA5, ITGA6, ITGA7, ITGA8, ITGAL, ITGAM, ITGAV, ITGB1, ITGB2, ITGB3, ITGB4, ITGB5, SGCE, SPP1, THBS3.
Other Adhesion Molecules: CNTN1, COL12A1, COL15A1, COL16A1, COL5A1, COL6A1, COL7A1, COL8A1, VCAN, CTGF, CTNNA1, CTNNB1, CTNND2, FN1, KAL1, LAMA1, LAMA2, LAMA3, LAMB1, LAMB3, LAMC1, THBS1, THBS2, CLEC3B, TNC, VTN.
Extracellular Matrix Proteins
Basement Membrane Constituents: COL4A2, COL7A1, LAMA1, LAMA2, LAMA3, LAMB1, LAMB3, LAMC1, SPARC.
Collagens & ECM Structural Constituents: COL11A1, COL12A1, COL14A1, COL15A1, COL16A1, COL1A1, COL4A2, COL3A1, COL5A1, COL6A1, COL6A2, COL7A1, COL8A1, FN1, KAL1.
ECM Proteases: ADAMTS1, ADAMTS13, ADAMTS8, MMP1, MMP10, MMP11, MMP12, MMP13, MMP14, MMP15, MMP16, MMP2, MMP3, MMP7, MMP8, MMP9, SPG7, TIMP1.
ECM Protease Inhibitors: COL7A1, KAL1, THBS1, TIMP1, TIMP2, TIMP3.
Other ECM Molecules: VCAN, CTGF, ECM1, HAS1, SPP1, TGFBI, THBS2, THBS3, CLEC3B, TNC, VTN, ELN.

The table has been modified from the gene table listed on http://www.sabiosciences.com/rt_pcr_product/HTML/PAHS-013A.html. See supplement table 3 for more details.

Supplement table 3: Detailed information of genes tested in modified ECM array

UniGene	RefSeq	Symbol	Description	Gene Name
Hs.643357	NM_006988	ADAMTS1	ADAM metallopeptidase with thrombospondin type 1 motif, 1	C3-C5, METH1
Hs.131433	NM_139025	ADAMTS13	ADAM metallopeptidase with thrombospondin type 1 motif, 13	ADAM-TS13, ADAMTS-13, C9orf8, VWFCP, vWF-CP
Hs.271605	NM_007037	ADAMTS8	ADAM metallopeptidase with thrombospondin type 1 motif, 8	ADAM-TS8, METH2
Hs.502328	NM_000610	CD44	CD44 molecule (Indian blood group)	CDW44, CSPG8, ECMR-III, HCELL, HUTCH-I, IN, LHR, MC56, MDU2, MDU3, MIC4, Pgp1
Hs.461086	NM_004360	CDH1	Cadherin 1, type 1, E-cadherin (epithelial)	Arc-1, CD324, CDHE, ECAD, LCAM, UVO
Hs.476092	NM_003278	CLEC3B	C-type lectin domain family 3, member B	TN, TNA
Hs.739161	NM_001843	CNTN1	Contactin 1	F3, GP135
Hs.523446	NM_080629	COL11A1	Collagen, type XI, alpha 1	CO11A1, COLL6, STL2
Hs.101302	NM_004370	COL12A1	Collagen, type XII, alpha 1	BA209D8.1, COL12A1L, DJ234P15.1
Hs.409662	NM_021110	COL14A1	Collagen, type XIV, alpha 1	UND
Hs.409034	NM_001855	COL15A1	Collagen, type XV, alpha 1	–
Hs.368921	NM_001856	COL16A1	Collagen, type XVI, alpha 1	447AA
Hs.681002	NM_000088	COL1A1	Collagen, type I, alpha 1	OI4
Hs.508716	NM_001846	COL4A2	Collagen, type IV, alpha 2	ICH, POREN2
Hs.210283	NM_000093	COL5A1	Collagen, type V, alpha 1	–
Hs.474053	NM_001848	COL6A1	Collagen, type VI, alpha 1	OPLL
Hs.420269	NM_001849	COL6A2	Collagen, type VI, alpha 2	PP3610
Hs.476218	NM_000094	COL7A1	Collagen, type VII, alpha 1	EBD1, EBDCT, EBR1
Hs.740613	NM_001850	COL8A1	Collagen, type VIII, alpha 1	C3orf7
Hs.410037	NM_001901	CTGF	Connective tissue growth factor	CCN2, HCS24, IGFBP8, NOV2
Hs.656653	NM_001903	CTNNA1	Catenin (cadherin-associated protein), alpha 1, 102kDa	CAP102
Hs.476018	NM_001904	CTNNB1	Catenin (cadherin-associated protein), beta 1, 88kDa	CTNNB, MRD19, armadillo
Hs.166011	NM_001331	CTNND1	Catenin (cadherin-associated protein), delta 1	CAS, CTNND, P120CAS, P120CTN, p120, p120(CAS), p120(CTN)
Hs.314543	NM_001332	CTNND2	Catenin (cadherin-associated protein), delta 2 (neural plakophilin-related arm-repeat protein)	GT24, NPRAP
Hs.81071	NM_004425	ECM1	Extracellular matrix protein 1	URBWD
Hs.203717	NM_002026	FN1	Fibronectin 1	CIG, ED-B, FINC, FN, FNZ, GFND, GFND2, LETS, MSF

UniGene	RefSeq	Symbol	Description	Gene Name
Hs.57697	NM_001523	HAS1	Hyaluronan synthase 1	HAS
Hs.643447	NM_000201	ICAM1	Intercellular adhesion molecule 1	BB2, CD54, P3.58
Hs.644352	NM_181501	ITGA1	Integrin, alpha 1	CD49a, VLA1
Hs.482077	NM_002203	ITGA2	Integrin, alpha 2 (CD49B, alpha 2 subunit of VLA-2 receptor)	BR, CD49B, GPIa, HPA-5, VLA-2, VLAA2
Hs.265829	NM_002204	ITGA3	Integrin, alpha 3 (antigen CD49C, alpha 3 subunit of VLA-3 receptor)	CD49C, GAP-B3, GAPB3, ILNEB, MSK18, VCA-2, VL3A, VLA3a
Hs.440955	NM_000885	ITGA4	Integrin, alpha 4 (antigen CD49D, alpha 4 subunit of VLA-4 receptor)	CD49D, IA4
Hs.505654	NM_002205	ITGA5	Integrin, alpha 5 (fibronectin receptor, alpha polypeptide)	CD49e, FNRA, VLA5A
Hs.133397	NM_000210	ITGA6	Integrin, alpha 6	CD49f, ITGA6B, VLA-6
Hs.524484	NM_002206	ITGA7	Integrin, alpha 7	–
Hs.171311	NM_003638	ITGA8	Integrin, alpha 8	–
Hs.174103	NM_002209	ITGAL	Integrin, alpha L (antigen CD11A (p180), lymphocyte function-associated antigen 1; alpha polypeptide)	CD11A, LFA-1, LFA1A
Hs.172631	NM_000632	ITGAM	Integrin, alpha M (complement component 3 receptor 3 subunit)	CD11B, CR3A, MAC-1, MAC1A, MO1A, SLEB6
Hs.436873	NM_002210	ITGAV	Integrin, alpha V (vitronectin receptor, alpha polypeptide, antigen CD51)	CD51, MSK8, VNRA, VTNR
Hs.643813	NM_002211	ITGB1	Integrin, beta 1 (fibronectin receptor, beta polypeptide, antigen CD29 includes MDF2, MSK12)	CD29, FNRB, GPIIA, MDF2, MSK12, VLA-BETA, VLAB
Hs.375957	NM_000211	ITGB2	Integrin, beta 2 (complement component 3 receptor 3 and 4 subunit)	CD18, LAD, LCAMB, LFA-1, MAC-1, MF17, MFI7
Hs.218040	NM_000212	ITGB3	Integrin, beta 3 (platelet glycoprotein IIIa, antigen CD61)	BDPLT16, BDPLT2, CD61, GP3A, GPIIIa, GT
Hs.632226	NM_000213	ITGB4	Integrin, beta 4	CD104
Hs.536663	NM_002213	ITGB5	Integrin, beta 5	–
Hs.521869	NM_000216	KAL1	Kallmann syndrome 1 sequence	ADMLX, HH1, HHA, KAL, KALIG-1, KMS, WFDC19
Hs.270364	NM_005559	LAMA1	Laminin, alpha 1	LAMA, S-LAM-alpha
Hs.200841	NM_000426	LAMA2	Laminin, alpha 2	LAMM
Hs.436367	NM_000227	LAMA3	Laminin, alpha 3	BM600, E170, LAMNA, LOCS, lama3a
Hs.650585	NM_002291	LAMB1	Laminin, beta 1	CLM, LIS5

UniGene	RefSeq	Symbol	Description	Gene Name
Hs.497636	NM_000228	LAMB3	Laminin, beta 3	BM600-125KDA, LAM5, LAMNB1
Hs.609663	NM_002293	LAMC1	Laminin, gamma 1 (formerly LAMB2)	LAMB2
Hs.83169	NM_002421	MMP1	Matrix metallopeptidase 1 (interstitial collagenase)	CLG, CLGN
Hs.2258	NM_002425	MMP10	Matrix metallopeptidase 10 (stromelysin 2)	SL-2, STMY2
Hs.143751	NM_005940	MMP11	Matrix metallopeptidase 11 (stromelysin 3)	SL-3, ST3, STMY3
Hs.709832	NM_002426	MMP12	Matrix metallopeptidase 12 (macrophage elastase)	HME, ME, MME, MMP-12
Hs.2936	NM_002427	MMP13	Matrix metallopeptidase 13 (collagenase 3)	CLG3, MANDP1
Hs.2399	NM_004995	MMP14	Matrix metallopeptidase 14 (membrane-inserted)	MMP-14, MMP-X1, MT-MMP, MT-MMP 1, MT1-MMP, MT1MMP, MTMMP1, WNCHRS
Hs.80343	NM_002428	MMP15	Matrix metallopeptidase 15 (membrane-inserted)	MT2-MMP, MTMMP2, SMCP-2
Hs.492187	NM_005941	MMP16	Matrix metallopeptidase 16 (membrane-inserted)	C8orf57, MMP-X2, MT-MMP2, MT-MMP3, MT3-MMP
Hs.513617	NM_004530	MMP2	Matrix metallopeptidase 2 (gelatinase A, 72kDa gelatinase, 72kDa type IV collagenase)	CLG4, CLG4A, MMP-II, MONA, TBE-1
Hs.375129	NM_002422	MMP3	Matrix metallopeptidase 3 (stromelysin 1, progelatinase)	CHDS6, MMP-3, SL-1, STMY, STMY1, STR1
Hs.2256	NM_002423	MMP7	Matrix metallopeptidase 7 (matrilysin, uterine)	MMP-7, MPSL1, PUMP-1
Hs.161839	NM_002424	MMP8	Matrix metallopeptidase 8 (neutrophil collagenase)	CLG1, HNC, MMP-8, PMNL-CL
Hs.297413	NM_004994	MMP9	Matrix metallopeptidase 9 (gelatinase B, 92kDa gelatinase, 92kDa type IV collagenase)	CLG4B, GELB, MANDP2, MMP-9
Hs.711235	NM_000615	NCAM1	Neural cell adhesion molecule 1	CD56, MSK39, NCAM
Hs.376675	NM_000442	PECAM1	Platelet/endothelial cell adhesion molecule	CD31, CD31, EndoCAM, GPIIA', PECA1, PECAM-1, endoCAM
Hs.82848	NM_000450	SELE	Selectin E	CD62E, ELAM, ELAM1, ESEL, LECAM2
Hs.728756	NM_000655	SELL	Selectin L	CD62L, LAM1, LECAM1, LEU8, LNHR, LSEL, LYAM1, PLNHR, TQ1
Hs.73800	NM_003005	SELP	Selectin P (granule membrane protein 140kDa, antigen CD62)	CD62, CD62P, GMP140, GRMP, LECAM3, PADGEM, PSEL
Hs.371199	NM_003919	SGCE	Sarcoglycan, epsilon	DYT11, ESG
Hs.111779	NM_003118	SPARC	Secreted protein, acidic, cysteine-rich (osteonectin)	ON

UniGene	RefSeq	Symbol	Description	Gene Name
Hs.185597	NM_003119	SPG7	Spastic paraplegia 7 (pure and complicated autosomal recessive)	CAR, CMAR, PGN, SPG5C
Hs.313	NM_000582	SPP1	Secreted phosphoprotein 1	BNSP, BSPI, ETA-1, OPN
Hs.369397	NM_000358	TGFBI	Transforming growth factor, beta-induced, 68kDa	BIGH3, CDB1, CDG2, CDGG1, CSD, CSD1, CSD2, CSD3, EBMD, LCD1
Hs.164226	NM_003246	THBS1	Thrombospondin 1	THBS, THBS-1, TSP, TSP-1, TSP1
Hs.371147	NM_003247	THBS2	Thrombospondin 2	TSP2
Hs.658188	NM_007112	THBS3	Thrombospondin 3	TSP3
Hs.522632	NM_003254	TIMP1	TIMP metallopeptidase inhibitor 1	CLGI, EPA, EPO, HCI, TIMP
Hs.633514	NM_003255	TIMP2	TIMP metallopeptidase inhibitor 2	CSC-21K, DDC8
Hs.644633	NM_000362	TIMP3	TIMP metallopeptidase inhibitor 3	HSMRK222, K222, K222TA2, SFD
Hs.734766	NM_002160	TNC	Tenascin C	150-225, DFNA56, GMEM, GP, HXB, JI, TN, TN-C
Hs.109225	NM_001078	VCAM1	Vascular cell adhesion molecule 1	CD106, INCAM-100
Hs.643801	NM_004385	VCAN	Versican	CSPG2, ERVR, GHAP, PG-M, WGN, WGN1
Hs.2257	NM_000638	VTN	Vitronectin	V75, VN, VNT
Hs.520640	NM_001101	ACTB	Actin, beta	BRWS1, PS1TP5BP1
Hs.534255	NM_004048	B2M	Beta-2-microglobulin	–
Hs.544577	NM_002046	GAPDH	Glyceraldehyde-3-phosphate dehydrogenase	G3PD, GAPD
Hs.412707	NM_000194	HPRT1	Hypoxanthine phosphoribosyltransferase 1	HGPRT, HPRT
Hs.546285	NM_001002	RPLP0	Ribosomal protein, large, P0	L10E, LP0, P0, PRLP0, RPP0
N/A	SA_00105	HGDC	Human Genomic DNA Contamination	HIGX1A
N/A	SA_00104	RTC	Reverse Transcription Control	RTC
N/A	SA_00104	RTC	Reverse Transcription Control	RTC
Hs.443625	NM_000090	COL3A1	Collagen, type III, alpha 1	EDS4A
Hs.647061	NM_000501	ELN	Elastin	SVAS, WBS, WS
N/A	SA_00103	PPC	Positive PCR Control	PPC
N/A	SA_00103	PPC	Positive PCR Control	PPC

Supplement table 4: ECM real time PCR array results

One-way ANOVA				
COMPARTMENT	**Gene name**	***p*-value**	**normal distribution?**	
EPIDERMIS	LAMA1	0.00833	yes	
DERMIS	HAS1	0.00268	yes	
	COL4A2	0.01259	yes	
	ITGA5	0.02301	yes	
	MMP1	0.03065	yes	
	MMP3	0.02659	yes	
Post-hoc Tukey's HSD testing				
COMPARTMENT	**Gene name**	***p*-value**	**Comparison**	**Effect**
EPIDERMIS	LAMA1	0.02063	NTSCAR-KSCAR	0.00374
		0.01016	NSKIN-NTSCAR	−0.00426
DERMIS	HAS1	0.01797	NSKIN-HTSCAR	0.00078
		0.00302	NSKIN-KSCAR	0.00106
		0.00589	NSKIN-NTSCAR	0.00095
	COL4A2	0.00804	NSKIN-KSCAR	0.39277
	ITGA5	0.01596	KSCAR-HTSCAR	−0.0651
	MMP1	0.04267	KSCAR-HTSCAR	184.601
	MMP3	0.02668	NSKIN-HTSCAR	0.10848
		0.0522	NSKIN-KSCAR	0.09419

The results of the PCR array of ECM-associated genes in the epidermis or dermis between skin equivalents of Nskin and various types of scar (NTscar, HTscar and Kscar). For analysis of the PCR data, gene expression ($2^{-\Delta Ct}$) was normalized with the geometric mean of two housekeeping genes (ACTB and HRPT1). Shapiro-Wilk normality tests confirmed the presence of a normal distribution, thus justifying the use of one-way ANOVA's to detect which genes showed significant differences between the four experimental groups. Post-hoc Tukey's HSD tests were performed for pair-wise comparisons. Differences were considered significant if $p<0.05$.